Journal of Minerals and Materials Characterization and Engineering, 2022, 10, 461-476
https://www.scirp.org/journal/jmmce
ISSN Online: 2327-4085
ISSN Print: 2327-4077

Chemical Characterization of Slags from an Old Smelter in Chihuahua, Mexico

Daphne Espejel-García*, Vanessa Verónica Espejel-García, Alejandro Villalobos-Aragón

Facultad de Ingeniería, Universidad Autónoma de Chihuahua, Chihuahua, México
Email: *despejel@uach.mx

How to cite this paper: Espejel-García, D., Espejel-García, V.V. and Villalobos-Aragón, A. (2022) Chemical Characterization of Slags from an Old Smelter in Chihuahua, Mexico. *Journal of Minerals and Materials Characterization and Engineering*, **10**, 461-476.
https://doi.org/10.4236/jmmce.2022.106033

Received: September 13, 2022
Accepted: October 16, 2022
Published: October 19, 2022

Abstract

Slag is waste from pyrometallurgical processing, usually stored in stacks or warehouses around or near smelters. Slag research has focused on potential environmental problems associated with slag weathering or processing for secondary metal recovery and/or other uses (construction, landscaping, etc.). Located in northern Mexico, the city of Chihuahua has a mining history that dates back to the eighteenth century. A lead smelter located southeast of Chihuahua City; closed in 1997, leaving behind a large pile of slag. In this study, a chemical analysis of smelter slag was carried out. The tailings contain Zn (15 - 35 wt%), Pb (0.5 - 4 wt%), As (0.6 wt%), Sn (888 ppb) and Hg (170 ppb). XRD identified several minerals such as hardystonite ($Ca_2ZnSi_2O_7$), melanotekite ($Pb_2Fe_2^{3+}(Si_2O_7)O_2$), kentrolite ($Pb_2Mn_2^{3+}(Si_2O_7)O_2$) and sphalerite (ZnS) in the glass. Major elements are present in phases such as monticellite ($CaMgSiO_4$), kirschsteinite ($CaFe^{2+}SiO_4$), hedenbergite ($CaFe^{2+}Si_2O_6$), babingtonite ($Fe_2Si_3O_9$), magnetite (Fe_3O_4), and calcite ($CaCO_3$). Whether the goal is reuse, recycling or remediation, research into the properties of slag and its environmental and health impacts (on vulnerable exposed populations) should continue to be relevant.

Keywords

Slag, Smelter, Contamination, Pyrometallurgical Processing

1. Introduction

Smelter slags are glassy residual waste materials considered as byproducts of the mining and steel industries [1], and their purpose is to trap the impurities and separate them from the metal. Slags are normally stored in large piles or stocks near the mines or smelter sites and are huge sources of waste if not properly re-

cycled and used [2]. Slags' research has focused on chemical characterization and environmental issues related to the weathering and recycling of slag dumps [3]. Slags have very particular physical and mechanical characteristics that make them suitable for a wide variety of applications. Uses of smelter slags include road building, railroad ballast, road base or sub-base material, in waste stabilization, various types of concrete aggregates, fill, glass manufacture and soil conditioning [1] [4] [5] [6]. Slags may occur in three different types: granulated, expanded, and air-cooled [7]. This project examines the geochemical characteristics and, as future work, leaching behavior of air-cooled slags located in a former smelter site in Chihuahua, Mexico.

The air-cooled slags are considered heterogeneous both in their mineralogy as in its chemical composition [8], generally, characterized by high metal and metalloid content due to technologies with inefficient metal recovery [9] [10]. In some cases, the content of metals in slags is similar or slightly higher than in mineral deposits from where they are extracted. Apart from being used as reuse aggregates, they are considered as materials where metals still can be extracted, problem is, the metallic elements are trapped within the glass and electro-or hydrometallurgical techniques are needed to extract them [10]. Slags solidify from incandescent material, so they crystallize a variety of minerals (silicates, carbonates, glass, etc.), and display textures as in rocks. Optical microscopy, ICP-MS, XRD, and SEM analyses, were used in this investigation to characterize the smelter slags.

Slags are attractive as a construction material due to its excellent geotechnical properties. However, in the environmental field, the concern has been spreading about the content and leaching of heavy metals, especially those that are harmful to health [11] [12] [13]; therefore, the physico-chemical characterization of materials is important to determine their use [14] [15]. Blast furnace slags are created when iron is made, producing raw materials such as raw iron ore, coke, lime, and limestone. The residual material that is known as blast furnace slag is defined by ASTM C-125 [16] [17] as "product not metallic consisting essentially of calcium silicates and aluminosilicates and other bases, developed in liquid conditions together with iron in blast furnaces" [7] [18] [19].

Blast furnace slags can be classified based on their origin: 1) granulated slags 2) expanded slags, and 3) air-cooled slags [7] [18] [19]. Granulated slags are created when the residual liquid is rapidly visualized with either water, air, or both, with a glassy material appearing with latent hydraulic properties and sand particle size. The expanded slags, like that the granulated ones cool rapidly, but expand due to the controlled amount of water, air, and steam. Air-cooled slags, as the name implies, cool to room temperature, solidifying at the same time as oxides, silicates, carbonates, or any other type of minerals along with glass, comprising both a glassy and crystalline texture [7] [13] [18] [19].

The chemical composition of blast furnace slags is expressed as following: 95% of silicon (Si), aluminum (Al), calcium (Ca) and magnesium (Mg) oxides, while the remaining 5% is composed of elements such as iron (Fe), lead (Pb), zinc

(Zn), among others. The specific chemical composition is according to the material's source [18]. Physical studies performed previously to air-cooled slags report densities from 2000 to 2500 kg·m^{-3} [20]. Slags produced in metal smelting processes are considered as chemically inert, since metals are associated with glass and silicate minerals and oxides, which have low solubility in water [21]. Blast furnace slags are also considered as a non-metallic product, essentially consisting of calcium silicates, and aluminosilicates, which developed in liquid conditions along with iron in the blast furnace [17].

One of the objectives of this project lies mainly in the evaluation of the physicochemical characteristics of the blast furnace slag obtained from the banks of foundry waste generated by an old smelting and refining company that operated in Chihuahua, in northern Mexico (**Figure 1**). Slags must be characterized both physically and chemically, but also, it is highly recommended to perform petrographic analysis (identification of mineral phases) to describe its texture, shape, and composition.

Blast Furnace Slags at a Former Smelter Plant in Chihuahua, Mexico

An old smelting plant is located within Chihuahua city, Mexico. The operating mining company, in its peak times produced a capacity of 120,000 tons of impure lead, silver, and gold; along with zinc oxides and cadmium oxides, which came from the Santa Eulalia, San Antonio, Parral, and Santa Bárbara mines, among others, all within the Chihuahua state [22]. The smelter plant operated since 1908 until 1997 when it stopped working [23]. The smelter site is located approximately 10 km SE of Chihuahua city's downtown; it used to be in the suburbs, but now is surrounded by housing complexes (**Figure 2**).

For over 80 years, the smelter plant processed large quantities of metal, which is equivalent to a large volume of waste material (slag) [23]. The slags can be used as a substitute building material, such as coarse aggregate in pavement bases. It should be noted that there are no physical or chemical studies reported in the available literature, that have been performed on slags produced at the old smelter plant in Chihuahua, Mexico.

Figure 1. Smelter slag material used for characterization.

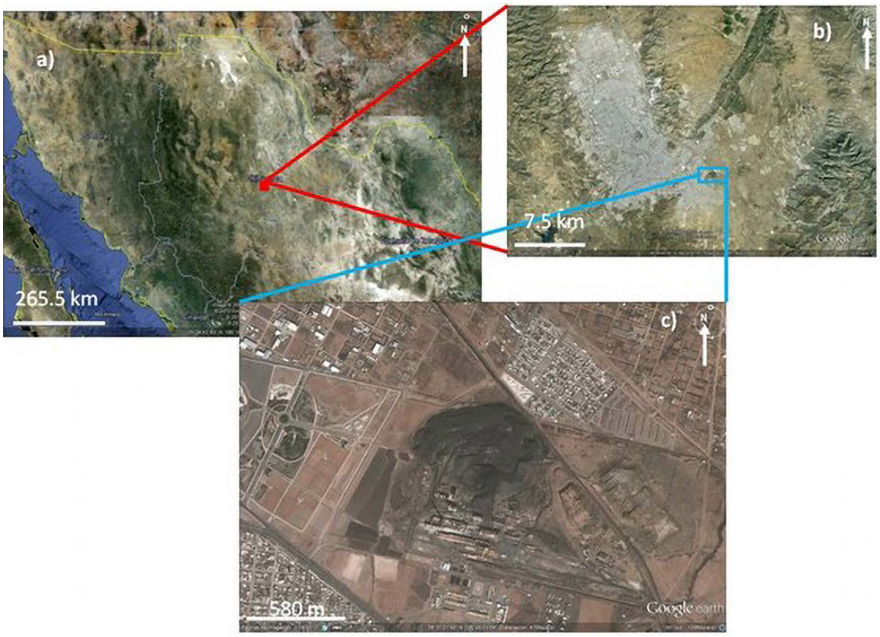

Figure 2. Location site of the former smelter in Avalos, Chihuahua, Mexico.

2. Materials and Methods

The first objective was to carry out a physicochemical characterization of the materials collected in the study site. Among the conventional tests performed were particle size analysis, maximum dry unit weight, relative density, absorption, degradation of small-size coarse aggregate by abrasion and impact, review of edges, etc. Additionally, analysis such as X-Ray diffraction (XRD), scanning electron microscopy (SEM), mass spectrometry (ICP-MS) and petrographic analysis, were performed.

2.1. Conventional Geotechnical Analyses

The base material meets all the requirements considered by the SCT (Ministry of Communications and Transportation in Mexico) quality standard N-CMT-4·02·002/04 [24], to be considered as pavement material, these requirements include:

1) Particle size of the material.

2) Atterberg limits (liquid and plastic limits).

3) Sand equivalent.

4) California Bearing Ratio (CBR).

5) Abrasion and impact in the Los Angeles machine test (ASTM C-131-06) [25].

6) Elongated and flaky particles.

7) Compaction quality control.

The blast furnace slag used in this analysis was subjected to several physical tests to learn more about their physical behavior.

The tests that were carried out on the slag were:

1) Maximum Dry Unit Weight of Coarse Aggregates

This test was carried out according to the American Society of Testing Materials Standard (ASTM C29/C29M-97) [26]. In this test, a container with a volume of 10 liters was used (0.01 m^3) and weighed in empty bascule. On a firm base the container was filled one third with the study material, leveling the surface. With the use of a bullet point rod (the end of a 5/8" steel rod spherically rounded), the layer filled with material is evenly tamped by distributing 25 blows over the layer. Next, the second third of the container is filled with the slag material and the material is tamped as described previously. Finally, the container is filled completely, and the material is tamped again. At the end of the filling of the container must be trimmed, so that the material is leveled with the surface of the container, once this is achieved, the container with the compacted material is weighted, thus using Equation (1):

$$\text{M.D.U.W.}\left(\text{kg}\cdot\text{m}^{-3}\right) = W_s / V_c \tag{1}$$

where:

M.D.U.W. = maximum dry unit weight ($kg\cdot m^{-3}$).

W_s = Sample's weight, obtained from obtained by subtracting the weight of the sample plus the container minus the container's weight (kg).

V_c = Volume of the container (m^3).

The test was performed in triplicate, to increase the precision of the results.

2) Relative Density and Absorption (Dr and Absorption)

The test was performed following the American Society of Testing Materials Std (ASTM C127-07) [27]. First, the slag was dried out in the sun's light and subsequently immersed in water for 24 hours. Once the material was saturated, it was extracted from water and placed on a damp absorbent flannel, removing the amount of surface water to obtain the saturated weight and superficially dried weights. This test requires the use of Archimedes' principle to obtain the volume dislodged from the material when immersed in water in a scale basket. After obtaining the saturated surface dried and submerged weights, the material is weighted again. The density relative and the absorption were calculated using Equation (2).

$$D_r = M_d / \left(V_r * \gamma_w\right) \tag{2}$$

where:

D_r = relative density.

M_d = Dry slag mass (g).

V_r = Real volume (cm^3), which was obtained from the subtraction of the dislodged volume minus the absorbed volume.

γ_w = Specific weight of water ($g\cdot cm^{-3}$).

Next, Formula (3) was used:

$$\text{Absorption} = \left(\left(W_{sss} - W_s\right)/W_s\right)\times 100 \tag{3}$$

with:

W_{sss} = Saturated and surficially dried slag weight (g).

W_s = Dried gravel weight (g).

3) Particle size analyses

The particle size distribution was obtained using the American Society of Testing Materials Standard (ASTM C33/C33M-11) [28]. In this study, slag material was considered as coarse, since its particles ranged from 0.18" (0.475 cm) up to 1.5", so the test procedure involved a mechanical analysis based on sieves with different openings such as: 2", 1.5", 1", 0.75", 0.5", 0.375", 0.25" and sieve number 4 (4.75 mm). Sieves were placed in descending order and a tray was placed at the end to capture the finest particles existing in the material. Subsequently, they were placed in a sieve vibrator, so that the material within go through the sieves until it is retained in the size where it no longer moved down. Once the vibration of the sieves ceased, the retained mass in each sieve was weighed, and the retained accumulated mass percentages were calculated. To obtain the passing material through each sieve, the accumulated percentage retained was subtracted from the 100% of the material used in the test. Finally, it is compared with **Table 2** of the ASTM C33/C33M-11 Std [28], to obtain the size number of the material.

4) Abrasion and impact test

This test measures the hardness property of aggregates, basically quantifies the resistance to degradation of small particles of the coarse-grained aggregate from abrasion and impact; this analysis is known as "Los Angeles Abrasion and impact Test". The standard used for this test was the one presented in the American Society of Testing Materials Manual (ASTM C131-06) [25]. The sample preparation was: 1) the material was dried with the sun light, and according to the particle size obtained in the previous tests, it was possible to determine the graduation and the number of 11 spheres to place inside the Los Angeles machine to start an impact process with 500 revolutions for every 5 kg of sample to be analyzed. Of those 5 kg used in the test, the half refers to material that passes the 3/4" mesh and is retained on the 1/2" mesh, and the other half is the material that passes the 1/2" mesh and is retained on the 3/8" mesh. Once the process ends in the Los Angeles machine, all the material (including the steel spheres) is removed. The remainder portion is sieved through the number 10 mesh (2.0 mm opening). The retained material is weighed in the sieve 10 and then Equation (4) is used.

$$\text{Aggregate Abrassion Value} = \left(\left(A - B\right)/A\right) \times 100 \tag{4}$$

with:

A = weight (g) of oved-dried sample.

B = weight (g) of fraction retained on sieve 10 after washing and oven-dried up to constant weight.

5) Optical analyses

- *Sphericity analysis*.

This is a visual test, representative slag aggregates were sampled to character-

ize its basic shape, since materials commonly reaccommodate and mix with particles of different sizes.

- *Slag thin sections*.

Three thin sections were made for analysis under the optical microscope, to describe and characterize petrographically the slags' mineral phases and textures. The thin sections were made by cutting the samples in slabs on a diamond blade cutter; these slabs were polished on a glass surface with a 500 abrasive and later glued to a glass thin section with Canada balsam. Before the balm dried, pressure was applied to the sample to eject any existing bubbles. Once the sample was well glued, it was devastated with a coarser abrasive (150), continued with the abrasive 800, and when it is very thin the sample was given the final polish with the abrasive 1200, until reaching an approximate thickness of 30 microns, the necessary measure to properly be observed under the microscope, because it is when the minerals show the appropriate colors.

2.2. Chemical Analyses

1) SEM analyses

Performed using Research Center of Advanced Materials' (CIMAV) Scanning Electron Microscope (SEM) Hitachi TM 4000 plus. The use of the SEM through the moving beam of electrons, allows the sample to be traversed or swept over selected areas, increasing the Image resolution of the smallest parts of materials. This equipment can obtain 3D images and transmit them to a computer monitor, thus performing morphological and chemical analyses of the material under study at the same time. One of the most used techniques in SEM analyses is imaging using secondary electrons, which are emitted from the solid sample by the ionizations that appear due to non-elastic interactions. With this technique, you get images of surface topographies. The use of backscattered electrons provides the topographic information with high depth contrast, that is, according to the colors that are perceived on the screen can be converted to accumulations of certain chemical compounds or elements in the sample. These backscatter electrons images provide higher contrast but lower resolution, when compared to those obtained by secondary electrons. Each point read within the sample equals one pixel on the screen, if the number of electrons is counted by the device increases, so will the brightness of the pixel on the screen [29].

2) X-ray Diffraction

To obtain the structural parameters of the samples under study, a finely grounded powder X-ray diffraction was obtained to confirm the phase using the Brag-Brentano technique. The analysis of the observed spectra was performed using a PANanalytical X'Pert PRO data collector, powder diffraction data interpretation and indexing software program X'Pert Highscore Plus. Version 2.2a. These analyses were performed at CIMAV's X-ray laboratory. XRD is a non-destructive technique used for identification and quantitative determination of various crystalline forms, known as phases of chemical compounds, present in solid

and powdered samples [30]. Identification is obtained by comparing the known X-ray diffraction pattern as a "diffractogram", which was obtained from an unknown sample with a database containing reference standards of more than 70,000 phases. Modern systems of computer-driven diffractometers use automated procedures to measure and interpret the diffractograms produced by the most complex elements and compounds.

3) Bulk Chemical Analyses by ICP-MS

The technique used for the chemical analysis of smelter slags, was by inductively coupled plasma mass spectrometry (ICP-MS). These analyses were carried out at the Activation Laboratories, LTD., in Canada.

3. Results and Discussion

Three representative slag samples were collected from the smelter site for bulk chemical analyses, thin sections, X-ray diffraction (XRD) analyses, SEM, and standard material tests.

3.1. Physical Properties

Physical property tests, such as abrasion, absorption, and relative density, were performed in the smelter slags, and the results are presented in average (**Table 1**).

3.2. Optical Analyses

1) Sphericity analysis

The representative samples analyzed, which included particles sizes from 1" to 1/2", have rounded edges, while particles smaller than 1/2" have angular edges, this is possibly due to the crushing in the slag pile (**Figure 3**).

2) Slag thin sections

The optical microscopy exposes different textures in the analyzed samples. Due to the rareness and small size of the minerals, these were identified using

Figure 3. Representative slag samples used to determine their sphericity.

Table 1. Physical parameters performed on slag material.

Maximum dry unit weight	2091.3 $kg \cdot m^{-3}$
Relative density (Dr)	3.46
Absorption	0.37%
Abrasion (according to ASTM C131-06)	13.11%

XRD analyses. Based on the observations, it can be said that the slags cooled down fast and are heterogeneous in composition. Mineral phases appear in different sizes and habits, suggesting changes in cooling velocities. The textures are not consistent, these variations can be explained from where the samples came from within the pile, the cooling velocities depended on whether the sample was near or far from the pile surface. The aphanitic texture (fine-grained) is the one that has more glass than minerals, which can trap the elements, making it more difficult to be released, being a key to interpret leaching experiments.

A description of each texture is provided next:

1) Sample SSA-01 (**Figure 4(a)**): Aphanitic and glassy texture. Opaque minerals (mgt) grow from a central point. Glass contains small silicate minerals.

2) Sample SSA-02 (**Figure 4(b)**): Porphyritic texture. 10% - 15% of euhedral/subhedral phenocrysts (coarse crystals). Sample include ferromagnesian and opaque minerals, calcite, and glass.

3) Sample S3 (**Figure 4(c)**): Medium grained spinifex-like texture. Minerals appear elongated pointing in different directions, and parallel with interstitial opaque minerals in between. Mineral crystallization appears skeletal.

3.3. SEM Analyses

SEM images (**Figure 5**) displayed at different scales, helped to described and determined the slags' textures and grains' habits (shape), portraying the heterogeneity of the material. As it can be observed, the slag surfaces can be porous, they have different mineralogy within a small area and occasionally appear in an agglutinated form.

3.4. Bulk Chemical Analyses

Quantitative analyses for four samples were performed in ICP-OES (**Table 2**). The samples report high values of iron (Fe), calcium (Ca), zinc (Zn), lead (Pb), silicon (Si) and magnesium (Mn), being the target of the leaching analyses (part of another research). Mercury (Hg) is also present in slags at values in ppb.

3.5. XRD Analyses

X-ray diffractograms (**Figure 6**) allowed to identify the following minerals included within the slags: silicates, carbonates, sulfides, and metal oxides (**Table 3**).

Silicates are mostly ferromagnesian, and phases with Mn, Ca, Pb and Zn. Calcite (carbonate) and magnetite (the only oxide phase) appear within the three

samples analyzed. Synthetic minerals, such as olivine and spinel, were found in these residual materials. S, Zn and Pb appear as elements or oxides, and can be considered as contaminants in water supply.

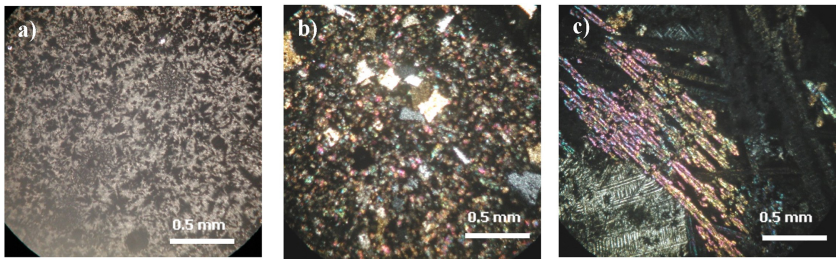

Figure 4. Photomicrographs of samples analyzed, in both Plane Polarized Light (PPL) and Crossed Polarized Light (XPL). (a) Sample SSA-01 with aphanitic (fine-grained) and glassy texture, image in PPL; (b) Sample SSA-02 with porphyritic texture (large crystals within a groundmass of fine crystals and glass), image in XPL; and (c) Sample SSA-03 with medium grained spinifex-like texture (minerals grew in elongated shapes), image in XPL.

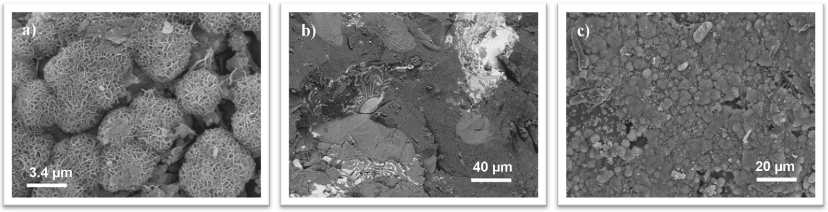

Figure 5. SEM images from analyzed samples. (a) Sample with porous texture; (b) Sample exhibiting different mineralogy within a small area, and (c) Sample that displays a globular texture or an agglutinated shape.

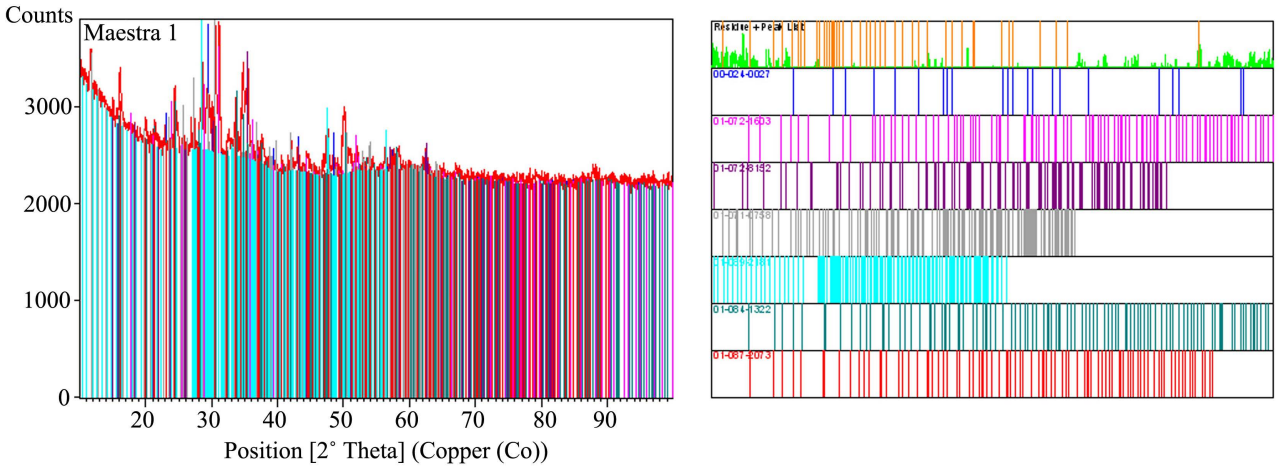

Pattern List

Visible	Ref.Code	Score	Compound Name	Displ.[°2Th]	Scale Fac.	Chem. Formula
*	00-024-0027	34	Calcite	-0.030	0.825	Ca C O3
*	01-072-1603	30	dicalcium zinc dis..	-0.027	0.665	Ca2 Zn Si2 O7
*	01-072-8152	40	iron diiron(III) o..	-0.005	0.783	Fe3 O4
*	01-071-0758	29	Ferrobustamite	0.044	0.910	(Ca0.79 Fe0.21) ..
*	01-089-2181	69	Zinc Sulfide	-0.053	0.739	Zn S
*	01-084-1322	32	Monticellite	-0.082	0.745	Ca Mg Si O4
*	01-087-2073	20	Kirschsteinite	0.213	0.431	Ca (Fe0.77 Mg0.22..

Figure 6. X-ray diffractogram and its interpretation from a selected sample.

Table 2. Representative bulk chemical analyses for slag samples.

Analyte Symbol	Unit Symbol	Detection Limit	Analysis Method	SLAG-01	SLAG-02	SLAG-03
SiO_2	%	0.01	FUS-ICP	28.97	28.94	28.31
Al_2O_3	%	0.01	FUS-ICP	3.05	3.01	2.77
Fe_2O_3 (T)	%	0.01	FUS-ICP	32.19	32.66	33.41
MnO	%	0.001	FUS-ICP	2.348	2.378	2.333
MgO	%	0.01	FUS-ICP	0.37	0.37	0.35
CaO	%	0.01	FUS-ICP	21.11	21.4	20.6
Na_2O	%	0.01	FUS-ICP	0.13	0.13	0.12
K_2O	%	0.01	FUS-ICP	0.46	0.45	0.37
TiO_2	%	0.001	FUS-ICP	0.156	0.154	0.145
P_2O_5	%	0.01	FUS-ICP	0.09	0.08	0.09
LOI	%	-	FUS-ICP	−2.91	−2.47	−1.49
Total	%	0.01	FUS-ICP	85.97	87.1	87.03
Sc	ppm	1	FUS-ICP	3	3	2
Be	ppm	1	FUS-ICP	7	7	7
V	ppm	5	FUS-ICP	107	107	94
Cr	ppm	20	FUS-MS	<20	<20	50
Co	ppm	1	FUS-MS	10	12	14
Ni	ppm	20	FUS-MS	<20	<20	<20
Cu	ppm	10	FUS-MS	1320	1310	2120
Zn	ppm	30	FUS-MS	>10,000	>10,000	>10,000
Ga	ppm	1	FUS-MS	18	19	19
Ge	ppm	1	FUS-MS	4	6	6
As	ppm	5	FUS-MS	196	383	457
Rb	ppm	2	FUS-MS	16	18	16
Sr	ppm	2	FUS-ICP	491	483	486
Y	ppm	2	FUS-ICP	10	10	<2
Zr	ppm	4	FUS-ICP	59	53	47
Nb	ppm	1	FUS-MS	4	3	4
Mo	ppm	2	FUS-MS	80	82	90
Ag	ppm	0.5	FUS-MS	10.9	17.6	9
In	ppm	0.2	FUS-MS	0.5	0.5	3
Sn	ppm	1	FUS-MS	595	712	888
Sb	ppm	0.5	FUS-MS	34.5	51.6	43.2

Continued

Cs	ppm	0.5	FUS-MS	1.5	1.5	1.4
Ba	ppm	3	FUS-ICP	788	802	760
La	ppm	0.1	FUS-MS	9.9	10.1	10.3
Ce	ppm	0.1	FUS-MS	17.1	17.1	17.1
Pr	ppm	0.05	FUS-MS	2.34	2.32	2.39
Nd	ppm	0.1	FUS-MS	8.8	8.6	9.2
Sm	ppm	0.1	FUS-MS	1.8	1.8	2
Eu	ppm	0.05	FUS-MS	0.42	0.45	0.46
Gd	ppm	0.1	FUS-MS	1.7	1.9	1.7
Tb	ppm	0.1	FUS-MS	0.3	0.3	0.3
Dy	ppm	0.1	FUS-MS	1.6	1.8	1.7
Ho	ppm	0.1	FUS-MS	0.3	0.3	0.3
Er	ppm	0.1	FUS-MS	0.9	1	1
Tm	ppm	0.05	FUS-MS	0.13	0.14	0.14
Yb	ppm	0.1	FUS-MS	0.9	0.9	0.9
Lu	ppm	0.04	FUS-MS	0.14	0.15	0.13
Hf	ppm	0.2	FUS-MS	1.3	1.2	1.3
Ta	ppm	0.1	FUS-MS	0.3	0.3	0.2
W	ppm	1	FUS-MS	85	81	79
Tl	ppm	0.1	FUS-MS	<0.1	<0.1	<0.1
Pb	ppm	5	FUS-MS	4710	6420	9010
Bi	ppm	0.4	FUS-MS	<0.4	<0.4	<0.4
Th	ppm	0.1	FUS-MS	3.2	3.2	3
U	ppm	0.1	FUS-MS	13.9	13.9	14.6
Hg	ppb	5	FUS-MS	258	132	119

Table 3. Physical parameters performed on slag material.

Mineral group	Name	Formula	Found in:		
			SSA-01	SSA-02	SSA-03
Silicates	Hardystonite	$Ca_2ZnSi_2O_7$	X	X	X
	Ferrobustamite	$Ca\ (Fe^{2+}, Ca, Mn^{2+})Si_2O_6$	X	X	X
	Monticellite (ol)	$CaMgSiO_4$	X	X	X
	Kirschsteinite	$CaFe^{+2}SiO_4$	X	X	
	Hedenbergite (px)	$CaFeSi_2O_6$		X	
	Pyroxferroite	$(Fe^{2+}, Mn^{2+}, Ca)SiO_3$		X	

Continued

	Babingtonite (px)	$Fe_2Si_3O_9$		X	
	Melanotekite	$Pb_2Fe_2^{3+}(Si_2O_7)O_2$			X
	Kentrolite	$Pb_2Mn_2Si_2O_9$			X
	Synthetic olivine	$MgMnSiO_4$			X
Oxides	Magnetite	Fe_3O_4	X	X	X
Sulfides	Sphalerite	ZnS	X	X	X
	Synthetic spinel *α*	$ZnAl_2S_4$		X	X
Carbonates	Calcite	$CaCO_3$	X	X	X
Elements	Zn, Pb, S		X	X	X
Other	Glass		X	X	

4. Conclusions and Future Work

Slags can be considered as a potential source of metals that, in the best-case scenario, could be reprocessed and obtain economic profit, but in the worst scenario, and thanks to weathering, the metals could be incorporated to soils, surface and/or groundwater, affecting the environment. To remove the large pile of slags concentrated in one spot, they can be employed as a substitute road material according to their physical properties, because they ensure greater resistance for any vehicle loads.

Any smelter slags must be physically and chemically characterized to be considered for reuse, since each smelter produced their own slags with their own characteristics. The smelter at Chihuahua City in northern Mexico, left piles of heterogeneous slags. The particles have different shapes, some rounded and some angular, depending on the size; different mineralogy including silicates, carbonates, oxides, sulfides, single elements, and glass. A variety of textures, such as aphanitic (fine-grained), porphyritic (coarse grains supported by fine grains and glass), and spinifex-like (elongated accumulation of grains), and the particles' surfaces are not smooth, they present porous textures and globular shapes. The slags physical properties conclude that can be used as aggregates, especially in the road building, because they have a high relative density (3.4), just 0.5 above the normal values of aggregates (2.4 - 2.9; ASTM C128-15) [31]; have low water absorption (0.37%), indicating a small amount of asphalt binder absorbed by the aggregates; and have a small percentage of abrasion (13%), being the permissible range from 30% to 60% (ASTM C131-06) [25], according to the type or road to be constructed.

If developers/governments plan in reusing the materials for sustainable construction, the slag can be combined with another natural resource such as: limestone, basalt, rhyolite, etc., reducing the vast amount of material used in road construction, and giving a reclaimed material a new use. The next stage in this research will be designing leaching experiments to determine if the waste prod-

ucts (slags) represent potential environmental issues when weathered. Results will be compared with drinking and industrial water norms to conclude whether these materials should be considered as a building material in road projects or as railroad ballast.

Acknowledgements

The authors would like to thank all the technical staff of the CIMAV's Microscopy, and X-ray Laboratories as well as UACH's Geology and Soils, Materials and Asphalts Laboratories for all their support.

Conflicts of Interest

The authors declare no conflicts of interest regarding the publication of this paper.

References

[1] Solomon, C.C. (1993) Annual Report Slag—Iron and Steel. US Department of the Interior, Bureau of Mines, Washington, D.C. https://d9-wret.s3.us-west-2.amazonaws.com/assets/palladium/production/mineral-pubs/iron-steel-slag/790494.pdf

[2] Reuter, M., Xiao, Y. and Boin, U. (2004) Recycling and Environmental Issues of Metallurgical Slags and Salt Fluxes. 7*th International Conference on Molten Slags Fluxes and Salts*, Johannesburg, 25-28 January 2004, 349-356. http://www.saimm.co.za/Conferences/MoltenSlags2004/349-Reuter.pdf

[3] Saikia, N., Borah, R.R., Konwar, K. and Vandecastelee, C. (2018) pH Dependent Leachings of Some Trace Metals and Metalloid Species from Lead Smelter Slag and Their Fate in Natural Geochemical Environment. *Groundwater for Sustainable Development*, **7**, 348-358. https://doi.org/10.1016/j.gsd.2018.01.009

[4] Pan, D.A., Li, L., Tian, X., Wu, Y., Cheng, N. and Yu, H. (2019) A Review on Lead Slag Generation, Characteristics, and Utilization. *Resources, Conservation and Recycling*, **146**, 140-155. https://doi.org/10.1016/j.resconrec.2019.03.036

[5] Babu, V., Kabeer, K.S.A. and Vyas, A.K. (2022) A Review on the Characterization and Use of ISF Slag as Fine Aggregate in Cement Concrete. *Materials Today: Proceedings*, **65**, 728-734. https://doi.org/10.1016/j.matpr.2022.03.281

[6] Reddy, N.G. and Rao, B.H. (2022) Physico-Chemical and Mechanical Characterization of Ferrochrome Slag Aggregates for Utilization as a Road Material. In: Tutumluer, E., *et al.*, Eds., *Advances in Transportation Geotechnics IV*, Vol. 164, Springer, Cham, 645-657. https://doi.org/10.1007/978-3-030-77230-7_49

[7] Puziewicz, J., Zainoun, K. and Bril, H. (2007) Primary Phases in Pyrometallurgical Slags from a Zinc-Smelting Waste Dump, Swietochłowice, Upper Silesia, Poland. *The Canadian Mineralogist*, **45**, 1189-1200. https://doi.org/10.2113/gscanmin.45.5.1189

[8] Parsons, M.B., Bird, D.K., Einaudi, M.T. and Alpers, C.N. (2001) Geochemical and Mineralogical Controls on Trace Element Release from the Penn Mine Base-Metal Slag Dump, California. *Applied Geochemistry*, **16**, 1567-1593. https://doi.org/10.1016/S0883-2927(01)00032-4

[9] Ettler, V., Legendre, O., Bodénan, F. and Touray, J.C. (2001) Primary Phases and Natural Weathering of Old Lead-Zinc Pyrometallurgical Slag from Príbram, Czech

Republic. *The Canadian Mineralogist*, **39**, 873-888.
https://doi.org/10.2113/gscanmin.39.3.873

[10] Lottermoser, B.G. (2002) Mobilization of Heavy Metals from Historical Smelting Slag Dumps, North Queensland, Australia. *Mineralogical Magazine*, **66**, 475-490.
https://doi.org/10.1180/0026461026640043

[11] Lind, B.B., Fällman, A.M. and Larsson, L.B. (2001) Environmental Impact of Ferrochrome Slag in Road Construction. *Waste Management*, **21**, 255-264.
https://doi.org/10.1016/S0956-053X(00)00098-2

[12] Xu, D.M., Fu, R.B., Tong, Y.H., Shen, D.L. and Guo, X.P. (2021) The Potential Environmental Risk Implications of Heavy Metals Based on Their Geochemical and Mineralogical Characteristics in the Size-Segregated Zinc Smelting Slags. *Journal of Cleaner Production*, **315**, Article ID: 128199.
https://doi.org/10.1016/j.jclepro.2021.128199

[13] Xu, D.M. and Fu, R.B. (2022) A Typical Case Study from Smelter-Contaminated Soil: New Insights into the Environmental Availability of Heavy Metals Using an Integrated Mineralogy Characterization. *Environmental Science and Pollution Research*, **29**, 57296-57305. https://doi.org/10.1007/s11356-022-19823-6

[14] Anove, K.M., Tchegueni, S., Degbe, K.A., Fiaty, K., Koriko, M., Drogui, P. and Tchangbedji, G. (2022) Physico-Chemical and Mineralogical Characterizations of Two Togolese Clays for Geopolymer Synthesis. *Journal of Minerals and Materials Characterization and Engineering*, **10**, 400-409.
https://doi.org/10.4236/jmmce.2022.105028

[15] Chamling, P.K., Haldar, S. and Patra, S. (2020) Physico-Chemical and Mechanical Characterization of Steel Slag as Railway Ballast. *Indian Geotechnical Journal*, **50**, 267-275. https://doi.org/10.1007/s40098-020-00421-7

[16] ASTM (2018) ASTM C125-Standard Terminology Relating to Concrete and Concrete Aggregates. ASTM International, West Conshohocken.

[17] Chesner, W.H., Collins, R.J., MacKay, M.H. and Emery, J. (2002) User Guidelines for Waste and By-Product Materials in Pavement Construction (No. FHWA-RD-97-148, Guideline Manual, Rept. No. 480017). Recycled Materials Resource Center, New Hampshire.

[18] Amaral de Lima, L. (1999) Hormigones con escorias de horno eléctrico de arco como áridos: propiedades, durabilidad y comportamiento ambiental. Doctoral Dissertation, Ph.D. Thesis, Universitat Politecnica de Catalunya, Barcelona. (In Spanish)

[19] Tossavainen, M., Engstrom, F., Yang, Q., Menad, N., Larsson, M.L. and Bjorkman, B. (2007) Characteristics of Steel Slag under Different Cooling Conditions. *Waste Management*, **27**, 1335-1344. https://doi.org/10.1016/j.wasman.2006.08.002

[20] Motz, H. and Geiseler, J. (2001) Products of Steel Slags an Opportunity to Save Natural Resources. *Waste Management*, **21**, 285-293.
https://doi.org/10.1016/S0956-053X(00)00102-1

[21] Piatak, N.M., Seal II, R.R. and Hammarstrom, J.M. (2004) Mineralogical and Geochemical Controls on the Release of Trace Elements from Slag Produced by Base- and Precious-Metal Smelting at Abandoned Mine Sites. *Applied Geochemistry*, **19**, 1039-1064. https://doi.org/10.1016/j.apgeochem.2004.01.005

[22] COREMI (1994) Consejo de Recursos Minerales. Monografía Geológico-Minera del Estado de Chihuahua. (In Spanish)

[23] Beltran, R. (2009) Fundición de Avalos: pilar de la economía por 84 años. El Heraldo de Chihuahua. (In Spanish)

https://avalosblog.wordpress.com/2009/06/17/fundicion-de-avalos-pilar-de-la-economia-por-84-anos

[24] SCT (1990) N-CMT-4·02·002/04 Características de los materiales (Materials' Characteristics), Secretaría de Comunicaciones y Transporte, México. (In Spanish) https://normas.imt.mx/normativa/N-CMT-4-02-002-20.pdf

[25] ASTM (2018) ASTM C131-06-Standard Test Method for Resistant to Degradation of Small-Size Coarse Aggregate by Abrasion and Impact in the Los Angeles Machine. ASTM International, West Conshohocken.

[26] ASTM (2018) ASTM C29-Standard Test Method for Bulk Density ("Unit Weight") and Voids in Aggregate. ASTM International, West Conshohocken.

[27] ASTM (2018) ASTM C127-07-Standard Test Method for Density, Relative Density (Specific Gravity), and Absorption of Coarse Aggregate. ASTM International, West Conshohocken.

[28] ASTM (2018) ASTM C33/C33M-11-Standard Specification for Concrete Aggregates. ASTM International, West Conshohocken.

[29] Zaefferer, S. (2011) A Critical Review of Orientation Microscopy in SEM and TEM. *Crystal Research and Technology*, **46**, 607-628. https://doi.org/10.1002/crat.201100125

[30] Suryanarayana, C. and Norton, M.G. (1998) X-Rays and Diffraction. In: Suryanarayana, C. and Grant Norton, M., Eds., *X-Ray Diffraction: A Practical Approach*, Springer, Boston, 3-19. https://doi.org/10.1007/978-1-4899-0148-4_1

[31] ASTM (2018) ASTM C128-15-Standard Test Method for Density, Relative Density (Specific Gravity), and Absorption of Fine Aggregate. ASTM International, West Conshohocken.